

Wall modeled large eddy simulation of the VFE-2 delta wing

Zwerger, C; Hickel, S.; Breitsamter, C; Adams, N

DOI

[10.1007/978-3-319-63212-4_36](https://doi.org/10.1007/978-3-319-63212-4_36)

Publication date

2018

Document Version

Final published version

Published in

Direct and Large-Eddy Simulation X

Citation (APA)

Zwerger, C., Hickel, S., Breitsamter, C., & Adams, N. (2018). Wall modeled large eddy simulation of the VFE-2 delta wing. In D. G. E. Grigoriadis, B. J. Geurts, H. Kuerten, J. Fröhlich, & V. Armenio (Eds.), *Direct and Large-Eddy Simulation X* (Vol. 24, pp. 289-295). (ERCOFTAC Series). Springer.
https://doi.org/10.1007/978-3-319-63212-4_36

Important note

To cite this publication, please use the final published version (if applicable).
Please check the document version above.

Copyright

Other than for strictly personal use, it is not permitted to download, forward or distribute the text or part of it, without the consent of the author(s) and/or copyright holder(s), unless the work is under an open content license such as Creative Commons.

Takedown policy

Please contact us and provide details if you believe this document breaches copyrights.
We will remove access to the work immediately and investigate your claim.

Wall Modeled Large Eddy Simulation of the VFE-2 Delta Wing

C. Zwerger, S. Hickel, C. Breitsamter and N. Adams

1 Introduction

Delta wing configurations are commonly employed for high agility supersonic aircraft and aerodynamic devices such as vortex generators, and have thus been a focus of extensive investigations over the past decades. A large data base of experimental and computational investigations is provided by the international vortex flow experiments VFE-1 and VFE-2, which constitute major collaborative efforts regarding these flows [4, 12]. Two aspects of the flow field are of particular interest: (1) leading edge bluntness effects on the primary vortex separation [14], and (2) vortex breakdown above the wing and its control [15]. The present study addresses both aspects.

With regard to aspect (1), the VFE-2 delta wing [2] with sharp leading edge (SLE) and medium radius round leading edge (MRLE) are investigated. The latter configuration is computationally more challenging than the sharp leading edge, since separation occurs closely behind the leading edge and is not geometrically fixed at the leading edge [14]. Numerical results are analyzed for three angles of attack α leading to different overall flow characteristics. For the MRLE and $\alpha = 13^\circ$, there is a partially developed primary vortex, starting approximately at one third chord length. For $\alpha = 18^\circ$, the primary vortex is fully developed for both leading edge geometries. For $\alpha = 23^\circ$, the primary vortex breaks down above the wing for both SLE and MRLE, the breakdown positions differ depending on the leading edge geometry, however.

C. Zwerger (✉) · S. Hickel · C. Breitsamter · N. Adams
Technische Universität München, Institute of Aerodynamics and Fluid Mechanics,
Boltzmannstr. 15, 85748 Garching, Germany
e-mail: christian.zwerger@tum.de

S. Hickel
Technische Universiteit Delft, Faculty of Aerospace Engineering,
Kluyverweg 2, 2629, HT Delft, The Netherlands

With regard to aspect (2), two possible flow control mechanisms are considered for the SLE and $\alpha = 28^\circ$: active flow control by oscillating control surfaces at the leading edges in the front part of the wing, and passive flow control by a geometric modification of the wing, leading to the injection of fluid from the pressure side.

RANS approaches, which are commonly used in industry, have shown only moderate success in investigations of the massively separated flow around a delta wing, notably regarding the correct prediction of vortex breakdown at high angles of attack [3, 5]. LES seems to be a more suitable approach for such flows, but is still prohibitively expensive when considering high-Reynolds number wall bounded flows. Therefore, we use wall modeled implicit large eddy simulation (WMLES), which relaxes the grid resolution requirements of LES close to walls. The influence of the wall model and different refinement levels of the grid are investigated.

For comparison we use experimental data available from measurements carried out at the Technische Universität München [6, 7, 13].

2 Numerical Approach and Setup

The implicit subgrid-scale model employed is based on the adaptive local deconvolution method (ALDM) [9, 10], and the wall model is based on the thin boundary layer equations (TBLE) [1]. For comparison we also performed LES with a simple no-slip boundary condition. The wing geometry [2] with root chord length $c_r = 1$ is mapped onto the Cartesian grid via a conservative immersed-interface method (CIIM) [8]. The computational domain is a cubic box with dimensions $-4 < x/c_r < 6$, $-5 < y/c_r < 5$, and $-5 < z/c_r < 5$. The wing tip is located at the point of origin. At the inflow, a uniform velocity profile is prescribed, and at the outflow, a static pressure of $P_{stat} = 1/(Ma^2 \cdot \gamma)$ is imposed, where Ma and γ denote Mach number and heat capacity ratio, respectively. Effects of wind tunnel walls are not simulated, and a slip condition is imposed at the remaining boundaries. The grids have been generated using an adaptive mesh refinement (AMR) technique. The cell size has been chosen such that the wall model coupling position lies within the logarithmic layer. Hereafter, results will be presented for two grids, denoted by Grid 1 and Grid 2. They are identical apart from the near wall region close to the apex, where Grid 2 is further refined. The grids had up to $74.2 \cdot 10^6$ cells. All investigations have been conducted for a Reynolds number based on the mean aerodynamic chord ($2/3 \cdot c_r$) of $Re = 2.0 \cdot 10^6$ and a Mach number of $Ma = 0.14$. Hereafter, if not otherwise specified, all quantities are nondimensionalized by free stream velocity U_∞ and root chord length c_r .

3 Results

With respect to leading edge bluntness effects, the numerical simulations predict the main flow phenomena qualitatively correctly for both leading edge geometries and for all angles of attack considered, see Fig. 1, leading to the characteristic pressure coefficient distribution with a suction peak below the axis of the primary vortex on the upper wing surface, see Fig. 2. However, there is no secondary vortex in any of the simulations due to the insufficient grid resolution, which does not allow for the prediction of such a small scale flow feature [11]. Quantitatively, the results show reasonable to good agreement with experimental measurements of steady (see Fig. 3) and unsteady surface pressures, velocity distributions, and vortex breakdown position and frequency. As expected, the agreement is overall better for the SLE due to the geometrically fixed separation at the leading edge. For the MRLE, the discrepancies between numerical and experimental results are largest in the apex region, where the leading edge crossflow bluntness, defined by the ratio of leading edge radius r_{le} and local half span width b_{loc} , is highest.

With respect to flow control, our numerical results show that oscillating control surfaces have only a minor effect on vortex breakdown, which is in agreement with experimental observations (Fig. 4). In the simulation, the vortex breakdown position was shifted from $x/c_r = 0.73$ to $x/c_r = 0.75$. Injecting fluid via the suggested geometric modification, however, significantly delays vortex breakdown. For this approach, the vortex breakdown position was shifted from $x/c_r = 0.73$ to

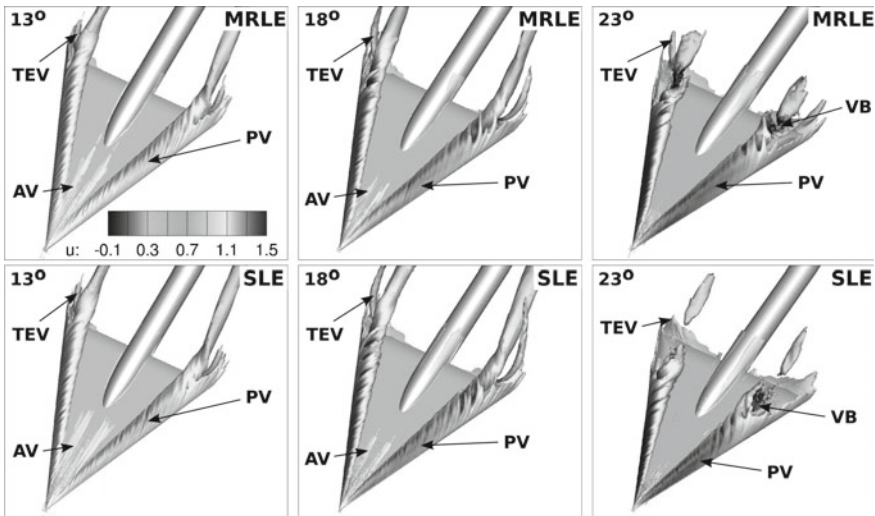


Fig. 1 Main flow characteristics at angles of attack of 13° (left), 18° (center), and 23° (right), obtained with Grid 1. AV - apex vortex, PV - primary vortex, TEV - trailing edge vortex, VB - vortex breakdown. *Top* and *bottom* row show isosurfaces of streamwise vorticity colored by streamwise velocity for MRLE and SLE, respectively

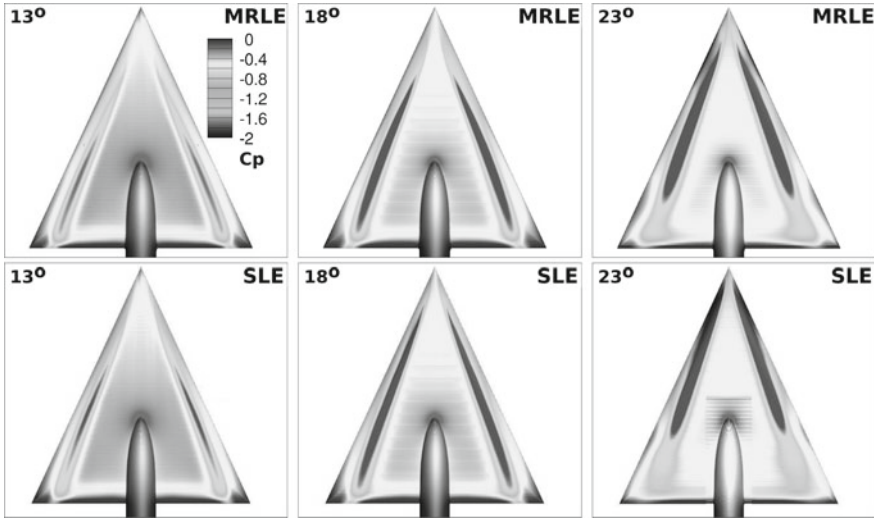


Fig. 2 Main flow characteristics at angles of attack of 13° (left), 18° (center), and 23° (right), obtained with Grid 1. Top and bottom row show surface pressure coefficient distributions for MRLE and SLE, respectively

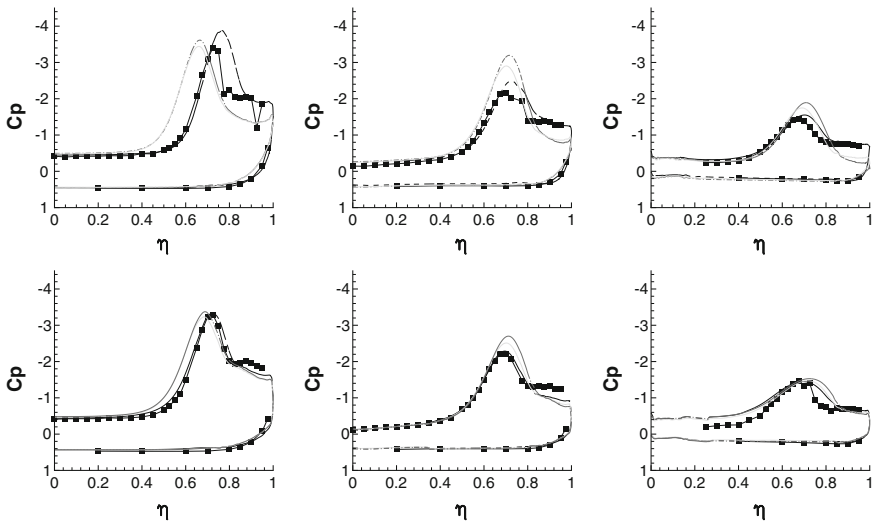


Fig. 3 Surface pressure distribution C_p at cross sections $x/c_r = 0.4, 0.6,$ and 0.8 (from left to right) for MRLE (top) and SLE (bottom) and $\alpha = 23^\circ$. Grid 1 with no-slip condition - dash-dotted; Grid 1 with TBLE wall model - solid; Grid 2 with no-slip condition - dashed; Experiments [6, 7] - solid with squares. η denotes normalized local half span width

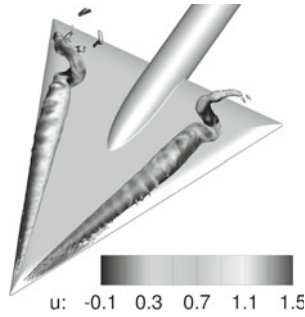


Fig. 4 Characteristic helical form of vortex breakdown. Rotation of vortex axis is opposite to rotation of primary vortex [12]. Figure shows isosurface of pressure coefficient ($C_p = -2$) colored by streamwise velocity for SLE and $\alpha = 23^\circ$

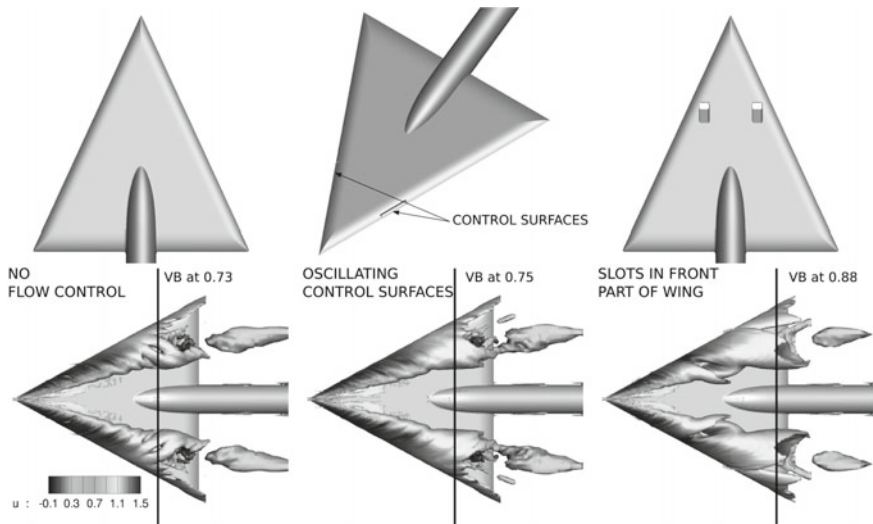


Fig. 5 No flow control (*left*), control surfaces in the front part of the wing (*center*), and slots in the front part of the wing (*right*). *Bottom row* figures show isosurface of streamwise vorticity colored by streamwise velocity. Vortex breakdown (VB) position indicated by *black line*

$x/c_r = 0.88$. Figure 5 shows the baseline configuration with no flow control (*left*), the configuration with oscillating control surfaces (*center*), and the configuration with a geometric modification (*right*), and the respective effects on the vortex breakdown position (*bottom row*).

4 Conclusion

We used wall modeled LES to investigate the flow field around the VFE-2 delta wing, focusing on (1) leading-edge bluntness effects and (2) vortex breakdown and its control.

With regard to (1) leading edge bluntness effects, our three main conclusions are: First, the main flow characteristics are predicted qualitatively correctly for all angles of attack and both SLE and MRLE, apart from the secondary vortex, which is not predicted due to the insufficient grid resolution. Second, quantitatively, the numerical predictions of velocity distributions, steady and unsteady surface pressures, and position and frequency of the vortex breakdown are overall in reasonable to good agreement with experimental data. Due to the geometrically fixed separation, the agreement is generally better for the SLE. Third, using a TBLE based wall model instead of a simple no-slip boundary condition leads only to a minor improvement of the results. However, refining the grid leads to a much more significant improvement suggesting that the TBLE based wall model contains too many approximations for the complex flow considered.

With regard to (2) vortex breakdown and its control, our two main conclusions are: First, flow control by oscillating control surfaces seems to have a minor impact on the vortex breakdown location for the configuration considered, which confirms experimental observations. Second, geometric modifications leading to the injection of fluid from the pressure side can have an effect resembling active blowing mechanisms and significantly delay vortex breakdown.

References

1. Chen, Z.L., Hickel, S., Devesa, A., Berland, J., Adams, N.A.: Wall modeling for implicit large-eddy simulation and immersed-interface methods. *Theor. Comput. Fluid Dyn.* **28**, 1–21 (2014)
2. Chu, J., Luckring, J.M.: Experimental surface pressure data obtained on 65° delta wing across reynolds number and mach number ranges. In: NASA technical memorandum 4645, vol. 3 - Medium-Radius Leading Edge (1996)
3. Crivellini, A., D'Alessandro, V., Bassi, F.: High-order discontinuous Galerkin RANS solutions of the incompressible flow over a delta wing. *Comput. Fluids* **88**, 663–677 (2013)
4. Drougge, G.: The international vortex flow experiment for computer code validation. In: ICAS-Proceedings, Jerusalem (1988)
5. Fritz, W., Cummings, R.M.: Lessons learned from the numerical investigations on the VFE-2 configuration. In: NATO STO, Summary Report of Task Group AVT-113, Chapter 34 (2009)
6. Furman, A., Breitsamter, C.: Experimental Investigations on the VFE-2 Configuration at TU Munich, Germany. In: NATO STO, Summary Report of Task Group AVT-113, Chapter 21 (2009)
7. Furman, A., Breitsamter, C.: Turbulent and unsteady flow characteristics of delta wing vortex systems. *Aerosp. Sci. Tech.* **24**, 32–44 (2013)
8. Grilli, M., Hickel, S., Hu, X.Y., Adams, N.A.: Conservative immersed boundary method for compressible viscous flows. In: Annual Report 2009 of the Sonderforschungsbereich/Transregio 40 (TRR40), Technische Universität München (2009)

9. Hickel, S., Adams, N.A., Domaradzki, J.A.: An adaptive local deconvolution method for implicit LES. *J. Comput. Phys.* **213**, 413–436 (2006)
10. Hickel, S., Egerer, C.P., Larsson, J.: Subgrid-scale modeling for implicit Large Eddy Simulation of compressible flows and shock turbulence interaction. *Phys. Fluids* **26**, 106101 (2014)
11. Hummel, D.: Effects of boundary layer formation on the vortical flow above slender delta wings. In: RTO symposium on enhancement of NATO military flight vehicle performance by management of interacting boundary layer transition and separation, Prague (2004)
12. Hummel, D.: The international vortex flow experiment 2 (VFE-2): objectives and overview. In: NATO STO, summary report of task group AVT-113, Chapter 17 (2009)
13. Kölzsch, A., Breitsamter, C.: Vortex-flow manipulation on a generic delta-wing configuration. *J. Aircr.* **51**, 1380–1390 (2014)
14. Luckring, J.M.: Initial experiments and analysis of blunt-edge vortex flows. In: NATO STO, summary report of task group AVT-113, Chapter 18 (2009)
15. Mitchell, A., Délyery, J.: Research into vortex breakdown control. *Prog. Aerosp. Sci.* **37**, 385–418 (2001)